HHS Public Access

Author manuscript

J Tissue Eng Regen Med. Author manuscript; available in PMC 2018 July 01.

Published in final edited form as:

J Tissue Eng Regen Med. 2017 July ; 11(7): 1963–1973. doi:10.1002/term.2093.

Ascorbic acid promotes extracellular matrix deposition while preserving valve interstitial cell quiescence within 3D hydrogel scaffolds

Yan Wu[1], **Daniel S. Puperi**[2], **K. Jane Grande-Allen**[2], and **Jennifer L. West**[1]

[1]Department of Biomedical Engineering, Duke University, Durham, NC, USA

[2]Department of Bioengineering, Rice University, Houston, TX, USA

Abstract

Current options for aortic valve replacements are non-viable and thus lack the ability to grow and remodel, which can be problematic for paediatric applications. Toward the development of living valve substitutes that can grow and remodel, porcine aortic valve interstitial cells (VICs) were isolated and encapsulated within proteolytically degradable and cell-adhesive poly(ethylene glycol) (PEG) hydrogels, in an effort to study their phenotypes and functions. The results showed that encapsulated VICs maintained high viability and proliferated within the hydrogels. The VICs actively remodelled the hydrogels via secretion of matrix metalloproteinase-2 (MMP-2) and deposition of new extracellular matrix (ECM) components, including collagens I and III. The soft hydrogels with compressive moduli of ~4.3 kPa quickly reverted VICs from an activated myofibroblastic phenotype to a quiescent, unactivated phenotype, evidenced by the loss of α-smooth muscle actin expression upon encapsulation. In an effort to promote VIC-mediated ECM production, ascorbic acid (AA) was supplemented in the medium to investigate its effects on VIC function and phenotype. AA treatment enhanced VIC spreading and proliferation, and inhibited apoptosis. AA treatment also promoted VIC-mediated ECM remodelling by increasing MMP-2 activity and depositing collagens I and III. AA treatment did not significantly influence the expression of α-smooth muscle actin (myofibroblast activation marker) and alkaline phosphatase (osteogenic differentiation marker). No calcification or nodule formation was observed within the cell-laden hydrogels, with or without AA treatment. These results suggest the potential of this system and the beneficial effect of AA in heart valve tissue engineering.

Keywords

VICs; ECM remodelling; phenotype; calcification; tissue engineering; scaffolds; PEG hydrogels

Conflict of interest

The authors have declared that there is no conflict of interest.

Supporting information

Description of methods for supplementary figures can be found in “Supplementary methods”

1. Introduction

Congenital pulmonary or aortic valve disease occurs in > 0.3% of births (Karamlou et al., 2005; Schoen, 2011). When valve reconstruction fails or is not feasible, valve replacement becomes inevitable. Although current options for valve replacements generally enhance survival and quality of life, they have severe limitations and are especially problematic for paediatric patients: mechanical valves require lifelong anticoagulation therapy; bioprothetic valves calcify rapidly in children (from months to years) (Husain and Brown, 2007; Schoen, 2011). Both mechanical and bioprosthetic valves are non-viable, which necessitates multiple valve replacement operations to implant larger valve substitutes as children grow, bringing significant dangers associated with repeat sternotomy (Andropoulos et al., 2002). Analysis of the outcomes of aortic valve replacement (either mechanical or bioprothetic valves) in 160 children showed that, within 10 years following replacement, 19% of patients died, 34% underwent a second replacement, and only 47% remained alive without the need for repeated replacement (Karamlou et al., 2005). An ideal valve substitute for these patients should be non-immunogenic, non-thrombogenic and capable of adaptive growth with growing patients, which has sparked interest in tissue-engineering approaches.

A significant challenge for tissue-engineered valve substitutes is to recapitulate the natural extracellular matrix (ECM) of the valve leaflets, including appropriate collagens, elastin, proteoglycans and glycosaminoglycans, since the ECM is largely responsible for the unique mechanical properties of the valve tissue. Valvular interstitial cells (VICs), the predominant cell population in valve leaflets, are responsible for active ECM synthesis in the valve tissue. Thus, stimulating VIC-mediated ECM synthesis in vitro is important to reconstruct valve composition and function. VICs are highly heterogeneous and dynamic in phenotype (Liu et al., 2007). In healthy adult valves, > 95% of VICs are quiescent, fibroblastic cells (Chen and Simmons, 2011; Rabkin-Aikawa et al., 2004). During valve injury or disease conditions, quiescent VICs can be activated into more contractile myofibroblasts, whose persistence may cause valve fibrosis (Chen and Simmons, 2011). VICs may also undergo osteogenic differentiation to form osteoblast-like cells that are associated with valve calcification (Monzack et al., 2009; Rodriguez and Masters, 2009), the leading valve disease in adults (Rodriguez et al., 2011). A tissue-engineering scaffold that supports and promotes VIC-mediated ECM remodelling while preserving their native, fibroblastic phenotype would be promising for constructing living valve substitutes.

Previous research has shown that maintenance of the VIC phenotype is highly sensitive to culture conditions. When cultured on standard tissue culture polystyrene plates in two dimensions (2D), VICs demonstrated an activated myofibroblast phenotype and elicited significant calcification (Benton et al., 2008). The quiescent, fibroblast phenotype of VICs was better preserved on the surface of soft poly(ethylene glycol) (PEG) hydrogels (Wang et al., 2013). However, previous work has shown that three-dimensional (3D) culture will promote cells to produce more physiologically relevant cellular responses in vitro (Griffith and Swartz, 2006). In some 3D studies, VICs were seeded on top of preformed meshlike synthetic (Andropoulos et al., 2002) or natural (Taylor et al., 2006) matrix scaffolds and left to migrate to the interior, which required culture times longer than a week. Although the optimization of scaffold properties, such as pore size and porosity, can promote cell

migration into the scaffold, time delay and uneven cell distribution are still an issue. Living cells can be homogeneously encapsulated inside hydrogels with cytocompatible crosslinking techniques. Cell-laden hydrogels have been developed from naturally derived molecules, i.e. collagen (Gould et al., 2012a, 2012b), hyaluronic acid (HA) (Masters et al., 2005; Rodriguez et al., 2011), fibrin (Flanagan et al., 2009; Mol et al., 2005) and synthetic polymers (PEG) (Shah et al., 2008). Most hydrogel-based research in heart valve tissue engineering has been performed with naturally derived materials, because of their easy access and important roles in native tissues. However, the inherent drawbacks of these materials (i.e. batch-to-batch variation, risk of inducing immunogenicity, and dimensional instability) have greatly limited their applications.

In contrast, PEG hydrogels are biocompatible and bioinert (West and Hubbell, 1999). They provide a blank slate to which bioactive molecules can be added to control cell–material interactions (Hahn et al., 2006; Hern and Hubbell, 1998; Hoffmann and West, 2010). The inclusion of cell-adhesive ligands and proteolytically degradable peptides allows control over cell attachment, spreading and ECM remodelling. Previous work by Benton et al. (2009) showed that VICs attained a spread morphology and proliferated in 3D PEG hydrogels. In that study, soluble transforming growth factor-β1 (TGFβ1) treatment increased the mRNA expression of collagen I, but also increased the expression of α-smooth muscle actin (αSMA), indicating myofibroblast differentiation (Benton et al., 2009). Although the collagen-promoting effect of TGFβ1 is promising, myofibroblast persistence may cause fibrosis. While some work has suggested that mechanical or biochemical stimuli can reduce overall cellular activation (Cushing et al., 2008; Wang et al., 2013), the development of platforms that limit or prevent long-term VIC myofibroblast activation would be ideal. Therefore, this study proposed to promote VIC-mediated ECM remodelling while preserving the cells' native quiescent, fibroblastic phenotype, in order to construct valve substitutes free from detrimental myofibroblast activation, osteogenic differentiation and calcification. In this study, 3D degradable and cell adhesive PEG hydrogels were used as a scaffold to support VIC growth. Cell adhesion was promoted by conjugating the fibronectin-derived RGDS peptide and proteolytic degradability of the hydrogel was enabled by incorporating a matrix metalloproteinase (MMP)-sensitive peptide.

In an effort to promote VIC-mediated ECM remodelling, the effects of ascorbic acid (AA) were also examined. AA, also known as vitamin C, is an essential nutrient acting as an anti-oxidant and co-factor for various enzymes, and thus has been used as a supplement for culture of various cell types. It has been reported to promote collagen secretion by smooth muscle cells and fibroblasts (Abe et al., 2001; Qiao et al., 2009) and to stimulate the proliferation of mesenchymal stem cells while preserving their differentiation ability (Choi et al., 2008). It also increases the replicative lifespan of endothelial cells (Shima et al., 2011). Furthermore, administration of AA shows beneficial effects against arterial dysfunction (Cangemi et al., 2007) and myocardial infarction (Ribeiro et al., 2009). However, little work has been conducted to understand its effect on VICs. Therefore, the effects of AA treatment on VIC phenotype, proliferation, apoptosis, MMP secretion and ECM deposition were investigated. The findings demonstrated the promotion of VIC-mediated ECM remodelling while preserving the quiescent fibroblastic phenotype, which can be beneficial in the development of tissue-engineered heart valves.

2. Materials and methods

All reagents were purchased from Sigma-Aldrich (St. Louis, MO, USA) unless otherwise indicated.

2.1. Cell isolation and culture

Primary VICs were harvested from aortic valve leaflets dissected out of fresh porcine hearts from a commercial abattoir (Fisher Ham and Meats, Spring, TX, USA). The leaflets were incubated with collagenase type II (550 U/ml, 30 min; Worthington Biochemical, Lakewood, NJ, USA), followed by manually scraping off endothelial cells and mincing the leaflets, which were then digested with collagenase type III (260 U/ml, 4 h; Worthington) in an incubated shaker (Stephens et al., 2007). Isolations from six different donors were pooled together to compensate for biological variability. The cells were cultured on tissue culture polystyrene flasks in growth medium [GM; 1:1 Dulbecco's modified Eagle's medium (DMEM; Corning, Tewksbury, MA, USA):F12 (Hyclone, Thermo Fisher Scientific, Waltham, MA, USA) with 10% bovine growth serum (BGS; Hyclone), 1.6% 1-m-4-(2-hydroxyethyl)-1- piperazine-ethanesulphonic acid (HEPES; Thermo Fisher Scientific) and 1% antibiotic–antimycotic solution (Lonza, Walkerville, MD, USA)] before being encapsulated. After encapsulation, cell-laden hydrogels were cultured in GM for 1 day and changed to different medium conditions, including GM, or GM supplemented with 50 μg/ml AA (GM + AA), or osteogenic medium (Osteo M; GM supplemented with 50 μg/ml AA, 10mM β-glycerophosphate disodium and 10 nM dexamethasone).

2.2. Synthesis and purification of PEG–PQ–PEG and PEG–RGDS

PEG–PQ–PEG and PEG–RGDS were synthesized, purified and characterized as previously described (Moon et al., 2010). Briefly, the MMP-2- and -9-sensitive peptide GGGPQGIWGQGK (PQ) was synthesized using a solid- phase peptide synthesizer (Aapptec, Louisville, KY, USA) via standard Fmoc chemistry, and characterized with MALDI–TOF MS (Applied Biosystems, Grand Island, NY, USA). This peptide was then reacted to heterobifunctional acrylate–PEG–succinimidyl valerate (PEG–SVA; Laysan Bio, Arab, AL, USA) at a molar ratio of 1:2 in 20mM HEPES buffer, pH8.3. The resultant PEG–PQ–PEG was then dialysed, lyophilized and stored at –20°C before use. PEG–RGDS was synthesized using a similar process by reacting the adhesive ligand RGDS (American Peptide, Sunnyvale, CA, USA) with PEG–SVA at a molar ratio of 1.2:1. Conjugation of peptides onto PEG chains was confirmed by gel permeation chromatography equipped with UV and evaporative light-scattering detectors (Varian, Palo Alto, CA, USA).

2.3. Cell encapsulation in hydrogels

Primary VICs between passages 2 and 4 were encapsulated within MMP-sensitive, cell-adhesive PEG hydrogels at a seeding density of 1×10^7 cells/ml. Briefly, hydrogel precursor solution was prepared with 4wt% PEG–PQ–PEG, 5 mM PEG–RGDS, 10 μM eosin Y, 1.5% v/v triethanolamine (TEOA) and 3.5 μl/ml N-vinylpyrrolidone (NVP) in 10 mM HEPES-buffered saline, pH 8.3. A 10 μl droplet of the precursor solution was sandwiched between a Sigmacoted glass slide and a methacrylate-modified glass coverslip, and photocrosslinked by white light exposure for 25s (Fibre-Lite Series 180, 150W halogen, Dolan Jenner,

Dayton, OH, USA), forming 380μm-thick hydrogel disks ('PEG–PQ' hydrogels). Cell-laden hydrogels were transferred to the indicated cell media and cultured at 37°C and 5% CO_2. Cell viability was assessed by calcein AM and ethidium homodimer staining (Live/Dead kit, Life Technologies, Grand Island, NY, USA) after maintaining in culture for 3days. Viability was quantified based on the top views of z-stacks covering a depth of 90 μm.

Methacrylate-modified glass coverslips were prepared by cleaning coverslips with 30% v/v hydrogen peroxide and 70% sulphuric acid and exposing to 2% 3-(trimethoxysilyl) propyl methacrylate in 95% ethanol overnight. The modified coverslips were rinsed with 95% ethanol and baked at 90 °C for 30 min before use.

2.4. Zymography

The conditioned media of cell-laden hydrogels (days 1–4) were collected and gelatin zymography was performed, using 10% Ready Gel Zymogram Gel (Bio-Rad, Hercules, CA, USA) to identify MMP secretion by encapsulated VICs. Protein standards (10–250 kDa; Bio-Rad) were used as ladders and fresh medium was used as a reference. Gel images were captured and band intensities were quantified using BioRad Image Lab software (n=4–5 hydrogels).

2.5.Immunohistochemistry

Cell-laden hydrogels were fixed with 4% paraformaldehyde (Electron Microscopy Sciences, Hatfield, PA, USA), permeabilized with 0.25% Triton X-100 and blocked with 3.5% bovine serum albumin (BSA; Fisher Scientific, Loughborough, UK) in phosphate-buffered saline (PBS; Corning; pH = 7.4). Samples were then incubated with primary antibodies against ki67 (at days 1, 7, 14 and 21; 1:50; Abcam, Cambridge, MA, USA), cleaved caspase-3 (day 28; 1:100; Cell Signaling Technology, Danvers, MA, USA), smooth muscle α-actin (αSMA; day 21; 1:100; Abcam) and alkaline phosphatase (ALP; day 28, 1:100, Abcam) in PBS. After rinsing three times with 0.01% Tween in PBS, with several hours/rinse, the samples were incubated with secondary antibodies: anti-rabbit IgG and anti-mouse IgG antibodies conjugated with either AlexaFluor 555 or AlexaFluor 647 (Life Technologies). Finally, to aid morphological analysis, actin and nuclei were stained with a 1:100 dilution of rhodamine phalloidin (Life Technologies) in 2μM DAPI. For collagen and elastin staining the same procedure was followed, with the exception of the permeabilization step. The primary antibodies used were anti-collagen I (Col I; day 28, 1:200; Abcam), anti-collagen III (Col III; day 28, 1:200; Abcam) and anti-elastin (1:50; Abcam). Fluorescent z-stacks were obtained on a confocal microscope (Zeiss LSM 510, Jena, Germany). z-Projections covering a depth of 80μm were obtained via ImageJ for visualization and quantitative analysis. Average z-projection area was calculated as the area covered by the z-projections of phalloidin divided by the numbers of DAPI-stained cell nuclei. Relative fluorescence was calculated by thresholding all channels uniformly and normalizing the mean fluorescent intensities of a specific channel to the corresponding DAPI channel by ImageJ. Eight z-stacks from three or four hydrogels were taken for quantification.

2.6. Cell proliferation and apoptosis

Cell proliferation was evaluated by measuring the change in cell number after encapsulation and culture. Cell-laden hydrogels were degraded using collagenase solution (250 U/ml, 10 min) and DNA content was measured using a Quant-iT PicoGreen dsDNA Kit (Life Technologies) and translated into cell numbers using a conversion factor of 5.6pg DNA/cell (see supporting information, Table S1). This conversion factor agrees closely with previously published data for VICs (Gregory, 2000; Munoz-Pinto et al., 2009). Cell proliferation was also characterized by immunostaining for the proliferation marker ki67, as described in the above section. Proliferation ratios were calculated by dividing proliferating cell numbers (counted from ki67-positive cells) to the total cell numbers (counted from DAPI channels) using the ImageJ 'Adjust Threshold' and 'Analyse Particles' functions.

Cell apoptosis was assessed with Caspase-Glo 3/7 Assay Kit (Promega, Madison, WI, USA) and caspase content was normalized to DNA content, as previously reported (Kumar et al., 2012). Briefly, on defined days (7, 14, 21 and 28), cell-laden hydrogels were degraded with collagenase solution (250 U/ml, 10 min). 100 μl of the degraded cell suspension were mixed with 100μl Caspase-Glo reagent with PicoGreen dye at a ratio of 1:200, and transferred to a 96-well plate. After incubation at room temperature for 30min, the total content of caspase 3 and 7 was determined by measuring luminescence and fluorescence (Promega; excitation 485 nm, emission 520 nm). Hydrogels without cells were used as the blank control in all the assays. Caspase content was calculated as luminescence (from caspase 3/7 assay) divided by fluorescence (from PicoGreen DNA assay) and normalized to that of blank hydrogels at each time point (n = 3–4 hydrogels).

2.7. Calcification

Xylenol orange (excitation 440, 570 nm, emission 610 nm) was used to detect calcium deposition by VICs. Samples were incubated in 50 μg/ml xylenol orange-supplemented media for 6h, followed by staining with DAPI and phalloidin.

2.8. Compression test

To avoid the influence of the underlying glass coverslips on the test of hydrogel stiffness, hydrogels with thickness of 1 mm were prepared and scraped off the coverslips for compression tests. The compressive properties of the hydrogel samples were tested using a Micro-strain analyser (TA Instruments RSA III, New Castle, DE, USA) under the Transient, Multiple Extension Mode. Compression tests were performed at a rate of 0.002 mm/s at room temperature. Compressive moduli were obtained from the linear part of the stress–strain curve, in the range 5–25% strain (n = 4–6 hydrogels).

2.9. Statistical analysis

Statistical analysis was performed using JMP 11 (SAS Institute Inc., Cary, NC, USA). The statistical significance of differences was determined by two-tailed Student's t-test without specifications; $p < 0.05$ was considered statistically significant. The proliferation and compression test studies were assessed by multi-factor ANOVA, followed by post hoc Tukey HSD. Results are reported as mean ± standard deviation (SD). For fluorescence

quantification, sample numbers were expressed as the numbers of hydrogels, whereas images taken from the same hydrogels were considered as replicates.

3. Results

3.1. VICs retain viability in 3D PEG–PQ hydrogels

VICs were encapsulated within 3D PEG–PQ hydrogels by mixing cells with the hydrogel precursor solution, followed by photocrosslinking. At day 3, the VICs were evenly dispersed within the hydrogels and approximately 98% of cells remained viable (Figure 1). AA treatment did not significantly influence cell viability (GM+AA, 0.976 ± 0.012 vs GM, 0.979 ± 0.006; n = 3; p = 0.81).

3.2. AA promotes cell spreading and MMP-2 secretion by VICs

One day after encapsulation within PEG–PQ hydrogels, the VICs started to demonstrate a spreading morphology in both GM and GM + AA groups (Figure 2A, B), and were homogeneously distributed through the PEG hydrogel thickness (Figure 2C, D). AA treatment increased the cell spread area within hydrogels by ~18% (Figure 2E).

Increased cell spreading in AA treatment group was consistent with the enhanced MMP-2 secretion by VICs in MMP-2-labile hydrogels. Zymography of cell culture supernatants (days 1–4) and the media control showed clear bands at MW ~68kDa, corresponding to MMP-2 (Figure 2F). Quantitative analysis of band intensity showed that the bands from cell culture supernatants were two to four times brighter than those in the media control, confirming new MMP-2 secretion by encapsulated VICs (Figure 2G). Also, bands at MW ~72 kDa appeared in cell culture supernatants, but not in the media control, indicating the secretion of pro-MMP-2 in cell culture (Figure 2F). Moreover, AA treatment enhanced MMP-2 secretion of encapsulated VICs by approximately 40% (Figure 2G).

3.3. AA promotes VIC growth and inhibits apoptosis

To evaluate the potential of cell-laden hydrogels to serve as a living tissue substitute and the effect of AA, cell proliferation and apoptosis of encapsulated VICs were assessed. Cell numbers increased by 33±16% in GM and by 76 ± 19% in GM + AA after 28 days of culture. Quantification of ki67 staining revealed that proliferation ratios in GM + AA were higher than those in GM at days 1 and 14 (20 ± 6% increase at day 1 and 19 ± 8% increase at day 14; n = 3; $p < 0.05$) (Figure 3A–C). These results confirmed the ongoing growth of the encapsulated VICs, which was further promoted by AA treatment.

Samples were immunostained for caspase-3 to estimate the cell population that underwent apoptosis. Only a small population (GM 3.3 ± 0.6% vs GM + AA 2.4 ± 0.6%; n = 3; p = 0.33) of encapsulated VICs underwent apoptosis (Figure 3D, E). The caspase 3/7 content, normalized to DNA, was consistently lower for GM + AA than for GM (60±3%, 43±7%, 63±3% and 66±8% decrease at days 7, 14, 21 and 28 days, respectively; n = 4; $p < 0.01$), indicating that AA inhibited apoptosis of encapsulated VICs (Figure 3F).

3.4. AA treatment enhances collagens I and III secretion by encapsulated VICs

VICs actively secreted collagens (Col) I and III, which were mainly pericellular. Comparing collagen secretion at different time points (Figure 4; see also supporting information, Figure S1), Col I and III secretion increased with culture time and began to organize into Col fibrils along the cell spreading direction. Moreover, AA treatment significantly increased Col I and III secretion by 113 ± 32% and 210 ± 18%, respectively, at day 28 ($n = 3$, $p < 0.01$). However, appreciable elastin deposition by VICs was not observed on either 2D glass substrate (10 days) or within 3D PEG–PQ hydrogels (30 days). The control porcine aortic smooth muscle cells (SMCs) secreted slightly more, but still extremely low, amounts of elastin under both conditions (see supporting information, Figure S4).

3.5. AA treatment does not affect the expression of αSMA and ALP

The expression of αSMA and alkaline phosphatase (ALP) was measured to evaluate VIC phenotype. VICs cultured on 2D glass chamber slides for 7 days were strongly positive for αSMA (see supporting information, Figure S2A, B). However, upon encapsulation within PEG–PQ hydrogels in GM for 1 day, ~(86 ± 4)% of VICs lost their expression of αSMA (see supporting information, Figure S2C). After culture in GM or GM+AA within PEG–PQ hydrogels for 21 days, the majority of VICs remained negative for αSMA staining (Figure 5A, B). ALP staining of VICs encapsulated within hydrogels for 28 days was diffuse and comparable in both groups (Figure 5C, D). The results of αSMA and ALP staining of VICs encapsulated in PEG–PQ hydrogels also revealed that AA treatment did not significantly influence the expression of these phenotype markers (Figure 5E; $n=3$; $p=0.30$).

3.6. AA treatment does not induce detrimental calcification

Xylenol orange (indicating calcification) was undetected in VIC-laden hydrogels cultured in GM or GM + AA for 28 days (Figure 6A, B), but in Osteo M it was faintly detectable in 3D hydrogels and strongly detectable on 2D glass chamber slides (positive control) (Figure 6C; see also supporting information, Figure S3).

3.7. Mechanical properties of cell-laden hydrogels maintain and enhance along with culture

As seen from Figure 7, the compressive moduli of cell-laden hydrogels at day 1 were lower than those of blank hydrogels without cells. Along with cell culture for 21 or 28 days, the compressive moduli of cell-laden hydrogels increased to a level not differentiable from those of blank hydrogels. AA treatment did not significantly change the compressive moduli of cell-laden hydrogels.

4. Discussion

The main finding of this study was that AA significantly enhanced Col I and III secretion by VICs, promoting VIC-mediated ECM remodelling. Col I and III secretion by VICs remained pericellular and began to organize along the direction of cell spreading (Figure 4), which may represent the preliminary formation of fibrillar collagen. Previous work showed that bundles of collagen fibres (mainly Col I and III) associate closely with VIC filopodia, forming a 3D superstructure in valve leaflets (Barth et al., 2009). These collagen fibres are

circumferentially aligned to provide tensile strength to withstand high-pressure loads (Vesely and Noseworthy, 1992). Therefore, we sought to promote Col I and III deposition by VICs in order to recapitulate the ECM components of the native valve tissue. AA acts as a co-factor in the post-translational modification of collagen molecules, and increases collagen production (Choi et al., 2008). The collagen-promoting effect of AA on VICs in this study was consistent with its effects on other cell types, such as smooth muscle cells and fibroblasts (Abe et al., 2001; Qiao et al., 2009).

AA also enhanced cell spreading and increased cell numbers. Cell adhesion and matrix degradation are necessary for cell spreading, migration and differentiation (Khetan and Burdick, 2010). The cell-adhesive ligand RGDS and an MMP-sensitive peptide were incorporated into PEG hydrogels to allow cell spreading and matrix degradation. The results showed that, besides the deposition of native ECM components (Figure 4), VICs also remodelled their surrounding matrix via MMP-2 secretion (Figure 2). MMP-labile hydrogels, in this case, provided temporary structural support. The course of scaffold degradation is highly dependent on the susceptibility of the cleavage sites and cellular activity. Thus, the control of degradation rate and profile can be achieved by either manipulating the susceptible segments (Deforest and Anseth, 2011; Patterson and Hubbell, 2010) or regulating cellular activities (Rabkin et al., 2001), allowing flexible design to match scaffold degradation and VIC-mediated ECM deposition. AA treatment increased MMP-2 secretion of VICs and thus promoted cell spreading (Figure 2). Moreover, VICs cultured in GM + AA showed higher proliferation ratios and lower apoptosis compared to those in GM (Figure 3). A similar proliferation-promoting effect of AA on other mesenchymal cell types was previously reported at low concentrations of AA (Choi et al., 2008; Takamizawa et al., 2004). However, high concentrations of AA or its derivatives may be cytotoxic and cause cell death (Choi et al., 2008). The mechanisms by which AA affects cell proliferation and apoptosis are not clear. It may mediate through reducing intracellular oxidative stress and regulating the synthesis of proteins related to cell growth (Shima et al., 2011). In this study, the enhanced proliferation and reduced apoptosis upon AA treatment led to a greater total cell number in GM + AA than that in GM. The increased total cell number, together with increased cell spreading, promoted the formation of cellular networks by VICs, leading to increased cell–matrix and cell–cell contacts. This is of critical importance, because cell–matrix and cell–cell communication determines cellular architectural organization, proliferation, differentiation and apoptosis (Latif et al., 2006). In native valves, VICs were recognized as a complex cellular network spanning the entire valve and comprising 30% of the valve's volume (Witt et al., 2012). Among the cellular network, VICs were connected by adherens junctions (Barth et al., 2009). Although the physiological significance of these junctions remains unclear, there is a possibility that VIC cellular networks may facilitate valve function by sensing physical forces and transmitting the information among cellular networks (Liu et al., 2007).

Although the characteristics of different VIC phenotypes and their roles in valve dysfuncion are still not fully understood, it is generally accepted that myofibroblast activation is characterized by significantly increased expression of αSMA, while osteogenic differentiation correlates with elevated expression of ALP and calcification (Rodriguez and Masters, 2009). VIC phenotypes are sensitive to substrate stiffness (Yip et al., 2009; Kloxin

et al., 2010; Wang et al., 2012; Duan et al., 2013; Quinlan and Billiar, 2012; Stephens et al., 2011; Gould et al., 2012a, 2012b) in addition to biochemical stimuli (Benton et al., 2009; Cushing et al., 2008). Culture of VICs on the surface of substrates of varying stiffness (0.15–154 kPa to the order of GPa) suggest that αSMA expression and organization increases with substrate stiffness (Quinlan and Billiar, 2012). Furthermore, reduction in substrate stiffness (E ~32 to ~7 kPa) could redirect VICs from activated myofibroblasts into a quiescent state (Kloxin et al., 2010; Wang et al., 2012). Although there is some discrepancy among reported threshold stiffness for myofibroblast activation of VICs [3.93 kPa (Duan et al., 2013) or 4.8–9.6 kPa (Quinlan and Billiar, 2012) or 7 kPa (Kloxin et al., 2010; Wang et al., 2012)], VICs cultured on soft substrates mimicking healthy valve fibrosa (0.5–5 kPa) maintain an unactivated phenotype. Therefore, in our study, hydrogel stiffness was designed to be close to 5 kPa to minimize myofibroblast activation. The results showed that the compressive moduli of cell-laden hydrogels were maintained throughout cell culture (E ~4.3 to ~6.0 kPa). Moreover, AA treatment did not significantly affect the compressive moduli of hydrogels, indicating the balanced effect of AA on cell-mediated hydrogel degradation and ECM deposition. Our findings in the VIC phenotype study showed that VICs on 2D glass chamber slides (moduli in the GPa range) were all strongly positive for αSMA (see supporting information, Figure S2A, B). However, upon encapsulation within 3D soft PEG hydrogels for 1day, the majority of VICs lost their expression of αSMA (see supporting information, Figure S2C) and remained negative after encapsulation for 21 days (Figure 5), resembling healthy adult valves, in which < 5% of VICs express αSMA (Duan et al., 2013). These findings implied that soft hydrogels quickly reverted VICs from an activated myofibroblastic phenotype to a quiescent phenotype in 3D. With regard to biochemical stimulation, previous work has largely focused on TGFβ1 treatment, demonstrating the promotion of collagen secretion, though it also upregulated the expression of αSMA, indicating myofibroblast activation (Benton et al., 2009). The upregulation of collagen secretion and ALP expression often coincide, leading to osteogenic differentiation and calcification (Lian and Stein, 1992). However, the upregulation of ALP expression also requires the cessation of proliferation (Abe et al., 2001). In this study, VICs maintained proliferation throughout the culture time of 4weeks, AA treatment further stimulated cell proliferation, and enhanced ALP expression was not observed. While the collagen-promoting effect is promising, phenotype preservation is also important, because VIC phenotype changes could cause progression toward valve diseases. No calcification was observed in cell-laden hydrogels cultured for 28 days, with or without AA (Figure 6), which was consistent with the healthy, fibroblastic phenotype of VICs. Therefore, in order to promote collagen deposition while preserving the quiescent, fibroblastic phenotype of VICs, AA shows promise for applications in heart valve tissue engineering.

A major challenge for heart valve tissue engineering is to understand VIC biology and pathology underlying valve diseases. This is difficult, due to the heterogeneous and dynamic nature of the cells, especially given the harvesting and plating onto 2D stiff polystrene substrates. Our system shows significant advantages for this work over the widely used, naturally derived materials. Naturally derived materials not only carry risks of inducing immune rejection, due to immunogenic remnants, but also suffer from poorly controlled cell–matrix interactions, due to batch-to-batch variation and the bioactive nature of these

molecules. For example, the hyaluronan fragments released from hyaluronan scaffolds can influence collagen and elastin secretion in a molecular weight-dependent manner (Masters et al., 2005; Shah et al., 2008), which renders it difficult to separate the influence of the biomaterial scaffold degradation from other factors in culture. The bioinert nature of PEG, with finely tunable bioactivity, provides an optimal platform to control the cell–matrix interactions and reliably study VICs' function and dysfunction. The results showed that VICs were homogeneously distributed within the hydrogels and ~98% of cells remained viable after encapsulation for 3 days (Figures 1 and 2), indicating the excellent cytocompatibility of our system. Compared to approaches where cells were seeded on a material's surface and penetrated via migration (Rabkin-Aikawa et al., 2004; Taylor et al., 2006), this in situ crosslinking technique achieved an even distribution of cells within the scaffolds. In addition, VIC growth and proliferation were supported for up to 4weeks in 3D hydrogels, showing the utility of these scaffold materials for long-term culture of VICs.

5. Conclusion

This study aimed to investigate the potential of cell-laden, proteolytically degradable PEG–PQ hydrogels to construct living valve substitutes that grow and remodel. The resulting 3D PEG–PQ hydrogels supported VIC adhesion, spreading, proliferation and ECM secretion for up to 4 weeks. Furthermore, AA promoted VIC growth and accelerated VIC-mediated ECM remodelling without inducing detrimental differentiation, which is potentially beneficial for the formation of living valve substitutes. Future work will focus on promoting the maturation of the cell-laden hydrogels into functional valve substitutes by optimizing the mechanical and biochemical cues from the hydrogels, such as substrate rigidity, anisotropy (Tseng et al., 2014) and growth factor stimuli.

Supplementary Material

Refer to Web version on PubMed Central for supplementary material.

Acknowledgements

This research was funded by the National Institutes of Health (NIH; Grant No. R01 HL107765). Special thanks to Maude Cuchiara, Melissa McHale and Liezl Balaoing for editorial assistance.

References

Abe T, Abe Y, Aida Y, et al. Extracellular matrix regulates induction of alkaline phosphatase expression by ascorbic acid in human fibroblasts. J Cell Physiol. 2001; 189:144–151. [PubMed: 11598899]

Andropoulos DB, Stayer SA, Skjonsby BS, et al. Anesthetic and perioperative outcome of teenagers and adults with congenital heart disease. J Cardiothorac Vasc Anesth. 2002; 16:731–736. [PubMed: 12486655]

Barth M, Schumacher H, Kuhn C, et al. Cordial connections: molecular ensembles and structures of adhering junctions connecting interstitial cells of cardiac valves in situ and in cell culture. Cell Tissue Res. 2009; 337:63–77. [PubMed: 19475424]

Benton JA, Fairbanks BD, Anseth KS. Characterization of valvular interstitial cell function in three-dimensional matrix metalloproteinase degradable PEG hydrogels. Biomaterials. 2009; 30:6593–6603. [PubMed: 19747725]

Benton JA, Kern HB, Anseth KS. Substrate properties influence calcification in valvular interstitial cell culture. J Heart Valve Dis. 2008; 17:689–699. [PubMed: 19137803]

Cangemi R, Angelico F, Loffredo L, et al. Oxidative stress-mediated arterial dysfunction in patients with metabolic syndrome: effect of ascorbic acid. Free Radic Biol Med. 2007; 43:853–859. [PubMed: 17664149]

Chen J-H, Simmons CA. Cell–matrix interactions in the pathobiology of calcific aortic valve disease: critical roles for matricellular, matricrine, and matrix mechanics cues. Circ Res. 2011; 108:1510–1524. [PubMed: 21659654]

Choi K-M, Seo Y-K, Yoon H-H, et al. Effect of ascorbic acid on bone marrow-derived mesenchymal stem cell proliferation and differentiation. J Biosci Bioeng. 2008; 105:586–594. [PubMed: 18640597]

Cushing MC, Mariner PD, Liao J-T, et al. Fibroblast growth factor represses Smad-mediated myofibroblast activation in aortic valvular interstitial cells. FASEB J. 2008; 22:1769–1777. [PubMed: 18218921]

Deforest CA, Anseth KS. Cytocompatible click-based hydrogels with dynamically tunable properties through orthogonal photoconjugation and photocleavage reactions. Nat Chem. 2011; 3:925–931. [PubMed: 22109271]

Duan B, Hockaday LA, Kapetanovic E, et al. Stiffness and adhesivity control aortic valve interstitial cell behavior within hyaluronic acid based hydrogels. Acta Biomater. 2013; 9:7640–7650. [PubMed: 23648571]

Flanagan TC, Sachweh S, Frese J, et al. In vivo remodeling and structural characterization of fibrin-based tissue-engineered heart valves in the adult sheep model. Tissue Eng A. 2009; 15:2965–2976.

Gould RA, Chin K, Santisakultarm TP, et al. Cyclic strain anisotropy regulates valvular interstitial cell phenotype and tissue remodeling in three-dimensional culture. Acta Biomater. 2012a; 8:1710–1719. [PubMed: 22281945]

Gould ST, Darling NJ, Anseth KS. Small peptide functionalized thiolene hydrogels as culture substrates for understanding valvular interstitial cell activation and de novo tissue deposition. Acta Biomater. 2012b; 8:3201–3209. [PubMed: 22609448]

Gregory TR. Nucleotypic effects without nuclei: genome size and erythrocyte size in mammals. Genome. 2000; 43:895–901. [PubMed: 11081981]

Griffith LG, Swartz MA. Capturing complex 3D tissue physiology in vitro. Nat Rev Mol Cell Biol. 2006; 7:211–224. [PubMed: 16496023]

Hahn MS, Miller JS, West JL. Three-dimensional biochemical and biomechanical patterning of hydrogels for guiding cell behavior. Adv Mater. 2006; 18:2679–2684.

Hern DL, Hubbell JA. Incorporation of adhesion peptides into nonadhesive hydrogels useful for tissue resurfacing. J Biomed Mater Res. 1998; 39:266–276. [PubMed: 9457557]

Hoffmann JC, West JL. Three-dimensional photolithographic patterning of multiple bioactive ligands in poly(ethylene glycol) hydrogels. Soft Matter. 2010; 6:5056–5063.

Husain AS, Brown JW. When reconstruction fails or is not feasible: valve replacement options in the pediatric population. Pediatr Card Surg Annu. 2007; 10:117–124.

Karamlou T, Jang K, Williams WG, et al. Outcomes and associated risk factors for aortic valve replacement in 160 children: a competing-risks analysis. Circulation. 2005; 112:3462–3429. [PubMed: 16316968]

Khetan S, Burdick JA. Patterning network structure to spatially control cellular remodeling and stem cell fate within three-dimensional hydrogels. Biomaterials. 2010; 31:8228–8234. [PubMed: 20674004]

Kloxin AM, Benton JA, Anseth KS. In situ elasticity modulation with dynamic substrates to direct cell phenotype. Biomaterials. 2010; 31:1–8. [PubMed: 19788947]

Kumar A, Wiltz DC, Grande-Allen KJ. Gentamicin reduces calcific nodule formation by aortic valve interstitial cells in vitro. Cardiovasc Eng Technol. 2012; 4:16–25. [PubMed: 25414733]

Latif N, Sarathchandra P, Taylor PM, et al. Characterization of molecules mediating cell–cell communication in human cardiac valve interstitial cells. Cell Biochem Biophys. 2006; 45:255–264. [PubMed: 16845172]

Lian JB, Stein GS. Concepts of osteoblast growth and differentiation: basis for modulation of bone cell development and tissue formation. Crit Rev Oral Biol Med. 1992; 3:269–305. [PubMed: 1571474]

Liu AC, Joag VR, Gotlieb AI. The emerging role of valve interstitial cell phenotypes in regulating heart valve pathobiology. Am J Pathol. 2007; 171:1407–1418. [PubMed: 17823281]

Masters KS, Shah DN, Leinwand LA, et al. Crosslinked hyaluronan scaffolds as a biologically active carrier for valvular interstitial cells. Biomaterials. 2005; 26:2517–2525. [PubMed: 15585254]

Mol A, van Lieshout MI, Dam-de Veen CG, et al. Fibrin as a cell carrier in cardiovascular tissue engineering applications. Biomaterials. 2005; 26:3113–3121. [PubMed: 15603806]

Monzack EL, Gu X, Masters KS. Efficacy of simvastatin treatment of valvular interstitial cells varies with the extracellular environment. Arter Thromb Vasc Biol. 2009; 29:246–253.

Moon JJ, Saik JE, Poche RA, et al. Biomimetic hydrogels with pro-angiogenic properties. Biomaterials. 2010; 31:3840–3847. [PubMed: 20185173]

Munoz-Pinto DJ, Jimenez-Vergara AC, Gelves LM, et al. Probing vocal fold fibroblast response to hyaluronan in 3D contexts. Biotechnol Bioeng. 2009; 104:821–831. [PubMed: 19718686]

Patterson J, Hubbell JA. Enhanced proteolytic degradation of molecularly engineered PEG hydrogels in response to MMP-1 and MMP-2. Biomaterials. 2010; 31:7836–7845. [PubMed: 20667588]

Qiao H, Bell J, Juliao S, et al. Ascorbic acid uptake and regulation of type I collagen synthesis in cultured vascular smooth muscle cells. J Vasc Res. 2009; 46:15–24. [PubMed: 18515971]

Quinlan AMT, Billiar KL. Investigating the role of substrate stiffness in the persistence of valvular interstitial cell activation. J Biomed Mater Res A. 2012; 100:2474–2482. [PubMed: 22581728]

Rabkin E, Aikawa M, Stone JR, et al. Activated interstitial myofibroblasts express catabolic enzymes and mediate matrix remodeling in myxomatous heart valves. Circulation. 2001; 104:2525–2532. [PubMed: 11714645]

Rabkin-Aikawa E, Farber M, Aikawa M, et al. Dynamic and reversible changes of interstitial cell phenotype during remodeling of cardiac valves. J Heart Valve Dis. 2004; 13:841–847. [PubMed: 15473488]

Ribeiro DA, Buttros JB, Oshima CTF, et al. Ascorbic acid prevents acute myocardial infarction induced by isoproterenol in rats: role of inducible nitric oxide synthase production. J Mol Histol. 2009; 40:99–105. [PubMed: 19466570]

Rodriguez KJ, Masters KS. Regulation of valvular interstitial cell calcification by components of the extracellular matrix. J Biomed Mater Res A. 2009; 90:1043–1053. [PubMed: 18671262]

Rodriguez KJ, Piechura LM, Masters KS. Regulation of valvular interstitial cell phenotype and function by hyaluronic acid in 2D and 3D culture environments. Matrix Biol. 2011; 30:70–82. [PubMed: 20884350]

Schoen FJ. Heart valve tissue engineering: quo vadis? Curr Opin Biotechnol. 2011; 22:698–705. [PubMed: 21315575]

Shah DN, Recktenwall-Work SM, Anseth KS. The effect of bioactive hydrogels on the secretion of extracellular matrix molecules by valvular interstitial cells. Biomaterials. 2008; 29:2060–2072. [PubMed: 18237775]

Shima N, Kimoto M, Yamaguchi M, et al. Increased proliferation and replicative lifespan of isolated human corneal endothelial cells with L-ascorbic acid 2-phosphate. Invest Ophthalmol Vis Sci. 2011; 52:8711–8717. [PubMed: 21980003]

Stephens EH, Carroll JL, Grande-Allen KJ. The use of collagenase III for the isolation of porcine aortic valvular interstitial cells: rationale and optimization. J Heart Valve Dis. 2007; 16:175–183. [PubMed: 17484468]

Stephens EH, Durst CA, West JL, et al. Mitral valvular interstitial cell responses to substrate stiffness depend on age and anatomic region. Acta Biomater. 2011; 9:7640–7650.

Takamizawa S, Maehata Y, Imai K, et al. Effects of ascorbic acid and ascorbic acid 2-phosphate, a long-acting vitamin C derivative, on the proliferation and differentiation of human osteoblast-like cells. Cell Biol Int. 2004; 28:255–265. [PubMed: 15109981]

Taylor PM, Sachlos E, Dreger SA, et al. Interaction of human valve interstitial cells with collagen matrices manufactured using rapid prototyping. Biomaterials. 2006; 27:2733–2737. [PubMed: 16406000]

Tseng H, Puperi DS, Kim EJ, et al. Anisotropic poly(ethylene glycol)/polycaprolactone hydrogel–fiber composites for heart valve tissue engineering. Tissue Eng A. 2014; 20:2634–2645.

Vesely I, Noseworthy R. Micromechanics of the fibrosa and the ventricularis in aortic valve leaflets. J Biomech. 1992; 25:101–113. [PubMed: 1733978]

Wang H, Haeger SM, Kloxin AM, et al. Redirecting valvular myofibroblasts into dormant fibroblasts through light-mediated reduction in substrate modulus. PLoS One. 2012; 7:e39969. [PubMed: 22808079]

Wang H, Tibbitt MW, Langer SJ, et al. Hydrogels preserve native phenotypes of valvular fibroblasts through an elasticity-regulated PI3K/AKT pathway. Proc Natl Acad Sci U S A. 2013; 110:19336–19341. [PubMed: 24218588]

West JL, Hubbell JA. Polymeric biomaterials with degradation sites for proteases involved in cell migration. Macromolecules. 1999; 32:241–244.

Witt W, Jannasch A, Burkhard D, et al. Sphingosine-1-phosphate induces contraction of valvular interstitial cells from porcine aortic valves. Cardiovasc Res. 2012; 93:490–497. [PubMed: 22232739]

Yip CYY, Chen J, Zhao R, et al. Calcification by valve interstitial cells is regulated by the stiffness of the extracellular matrix. Arterioscler Thromb Vasc Biol. 2009; 29:936–942. [PubMed: 19304575]

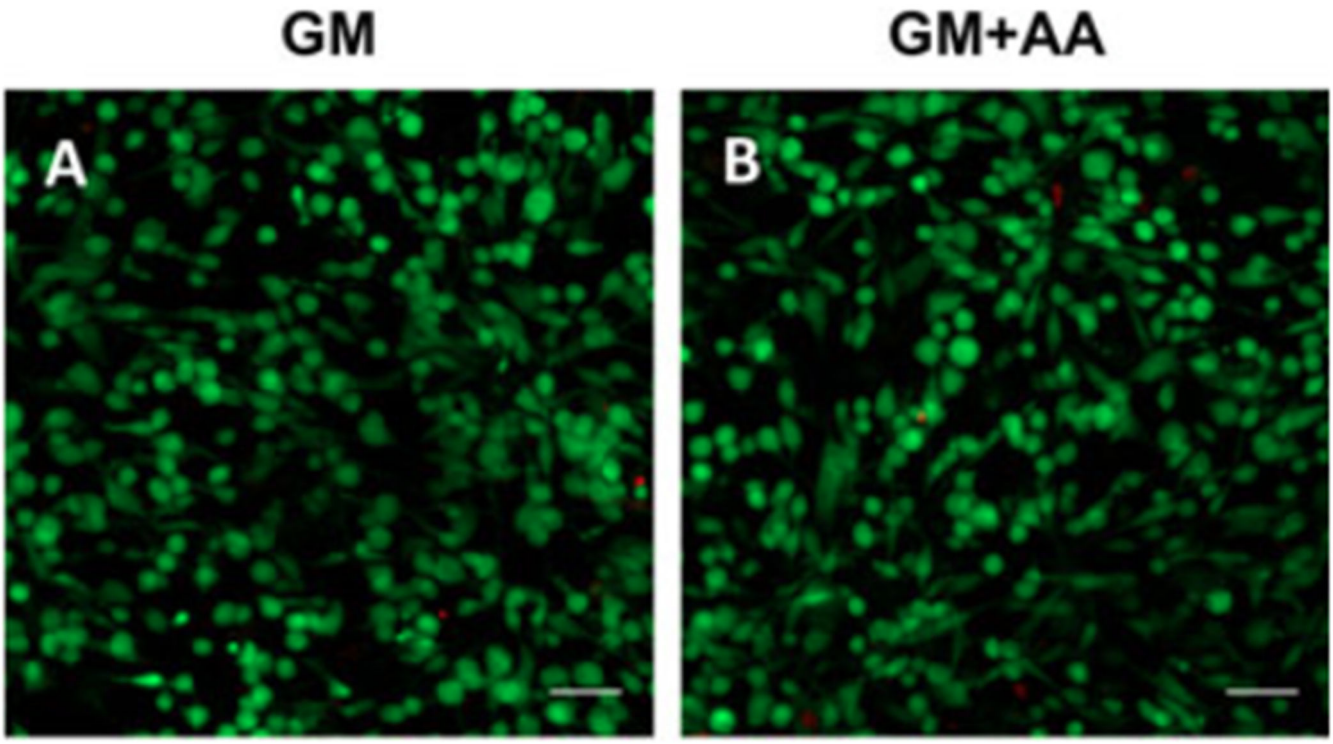

Figure 1.

VICs remained viable when encapsulated in PEG–PQ hydrogels for 3days. Representative images of cell-laden hydrogels stained with calcein AM (green, live) and ethidium homodimer (red, dead) cultured in (A) GM or (B) GM + AA; scale bars=50μm

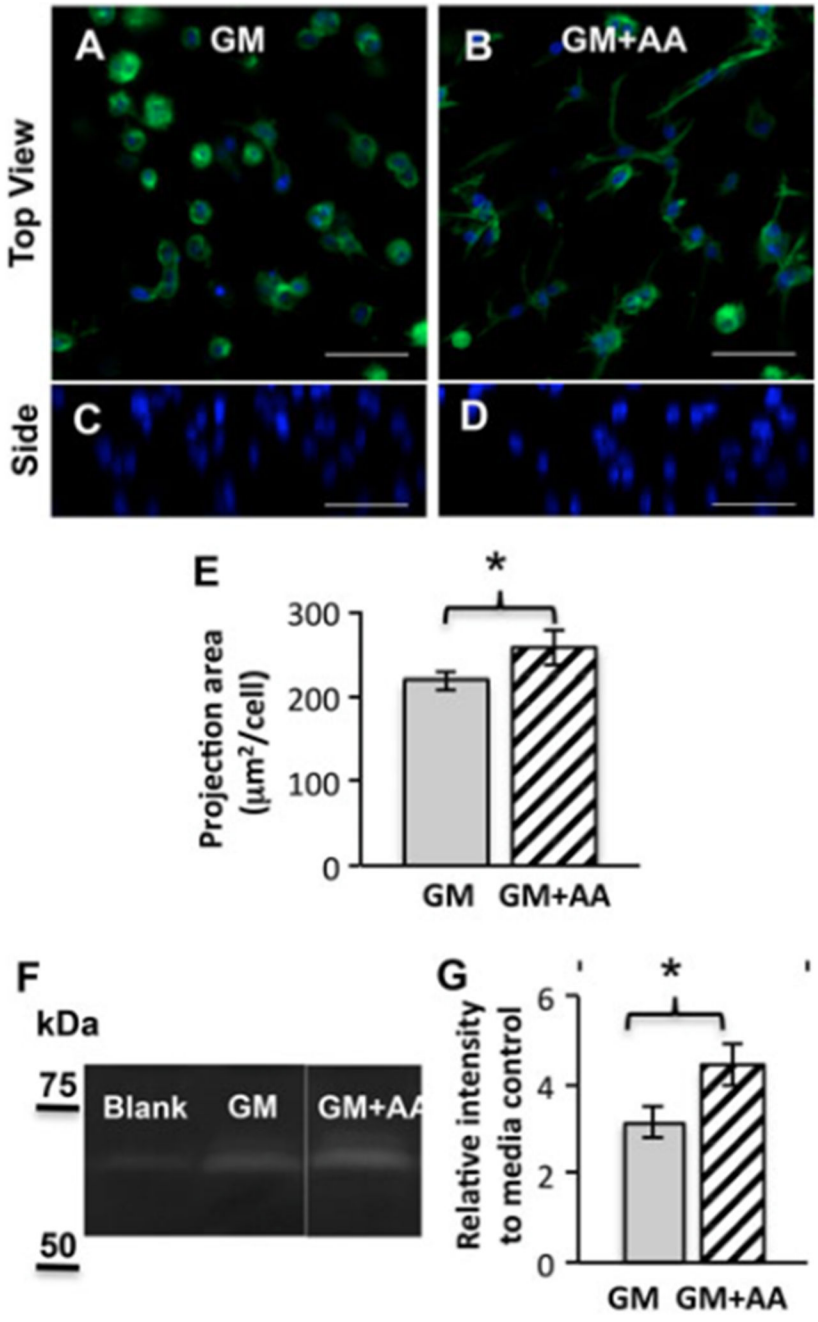

Figure 2.

AA promotes cell spreading and MMP-2 secretion within MMP-labile PEG–PQ hydrogels. (A–D) Representative images of cell spreading within hydrogels after encapsulation for 1 day in (A, C) GM or (B, D) GM + AA; blue (DAPI), nuclei; green (phalloidin), actin; top (A, B) and side (C, D) views; scale bars=50μm. (E) Average z-projection area of VIC spreading within hydrogels at day 1; *$p < 0.05$; $n = 3$. (F–G) Zymography of fresh media control and conditioned media collected from encapsulated VIC culture (days 1–4): (F)

Representative image of zymography with clear bands corresponding to MMP-2; (G) Quantitative analysis of band intensities relative to the media control; *$p<0.01$; n=4–5

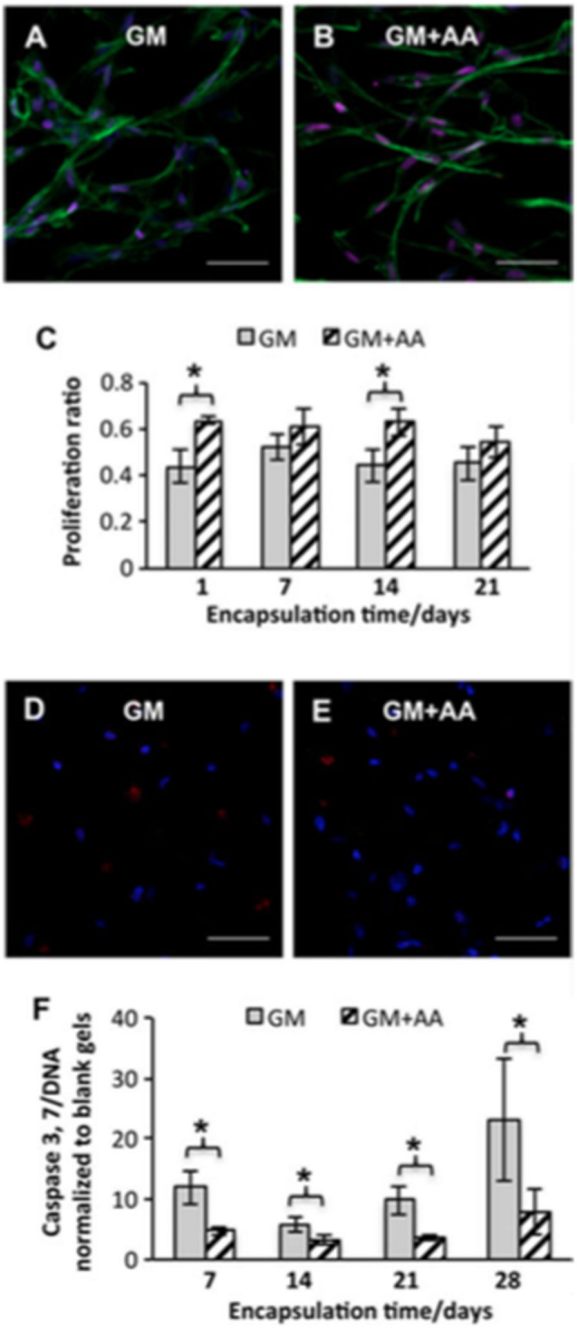

Figure 3.

AA treatment enhanced cell proliferation and inhibited apoptosis. (A–C) ki67 staining of VICs encapsulated in PEG hydrogels for 21 days: representative fluorescent images of (A) cell-laden hydrogels in GM or (B) GM+AA: red, ki67; blue (DAPI), nuclei; green (phalloidin), actin. (C) Quantitative analysis of proliferation ratios;*$p < 0.05$; $n = 3$. (D, E) Representative images of caspase-3 staining of cell-laden hydrogels cultured in (D) GM or (E) GM + AA for 28 days: red, caspase-3; blue (DAPI), nuclei; scale bars = 50 μm. (F)

Relative caspase content of VICs cultured in GM and GM + AA normalized to that of blank gels without cells; *$p < 0.01$; $n = 4$

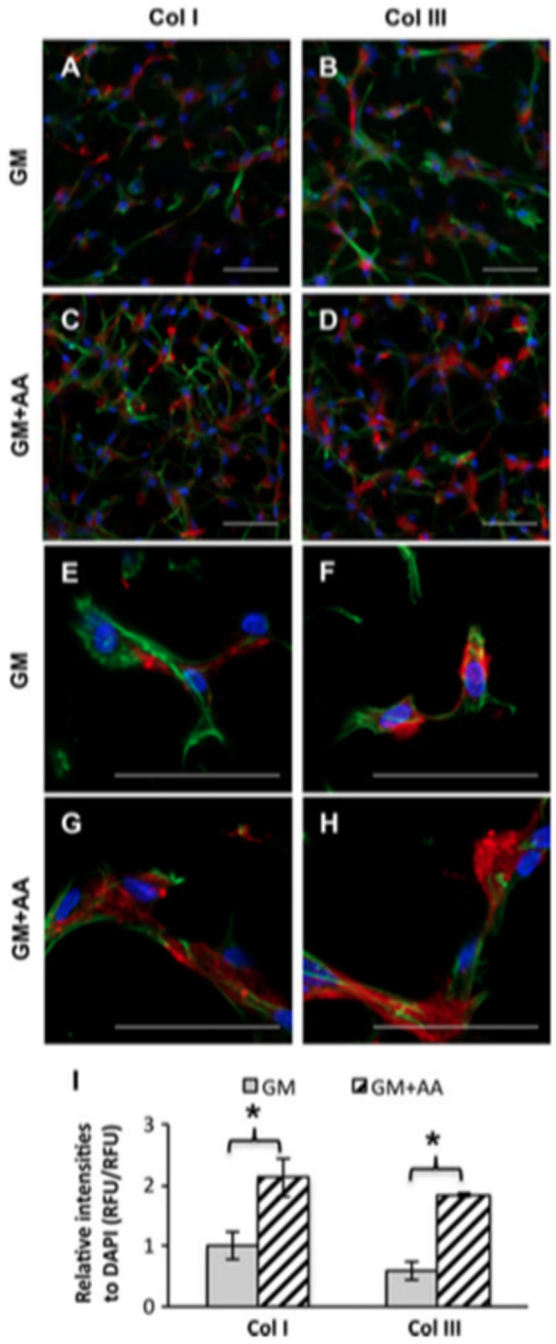

Figure 4.

AA treatment enhanced Col I and III secretion by VICs encapsulated in PEG–PQ hydrogels for 28 days. (A–H) Representative fluorescent images of Col I and Col III staining: red, Col I or III; blue (DAPI), nuclei; green (phalloidin), actin; (A, E) Col I, GM; (B, F) ColIII, GM; (C,G) ColI, GM+AA; (D,H) ColIII, GM+AA; scale bars = 50 μm. (I) Quantitative analysis based on relative fluorescence intensities of Col I, Col III and DAPI; *$p < 0.01$, $n = 3$

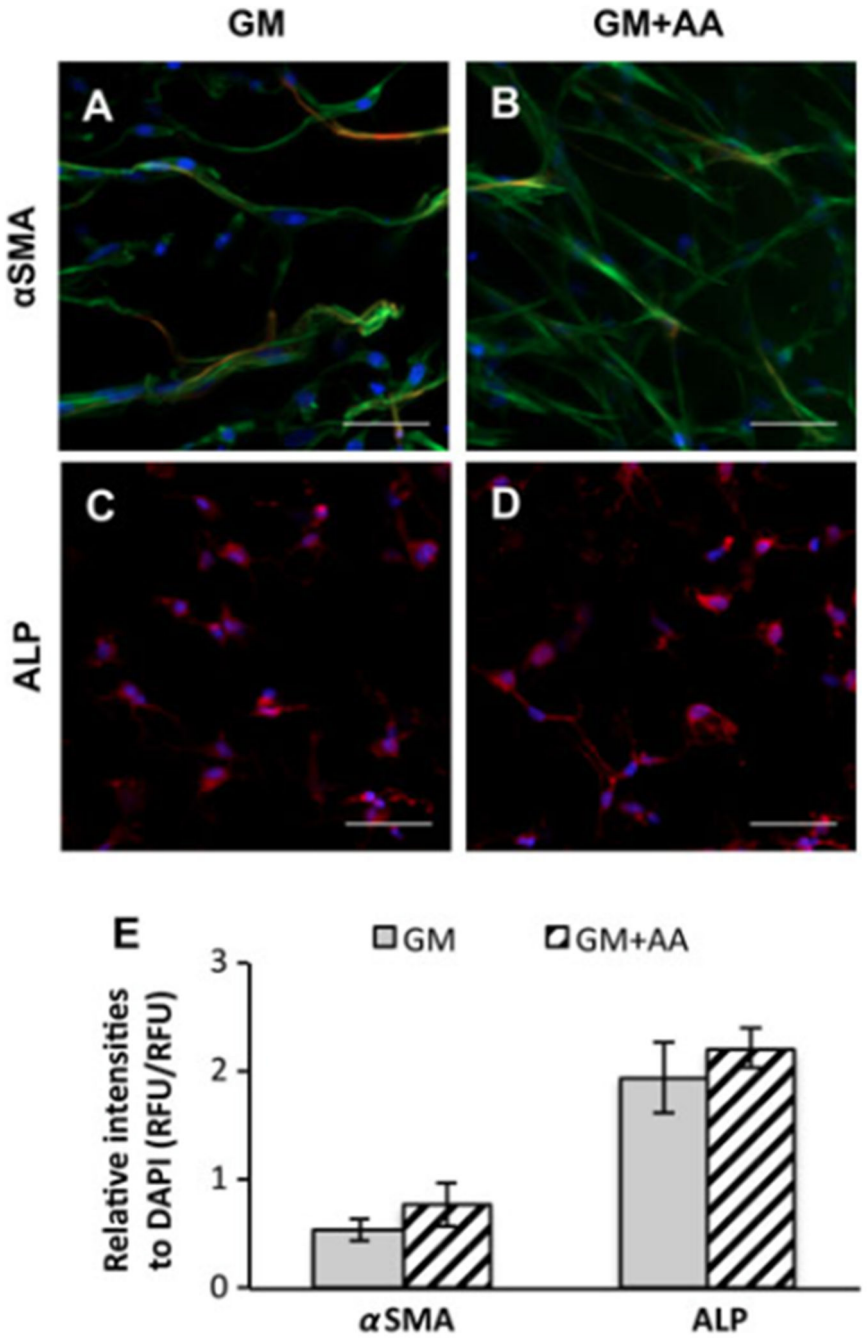

Figure 5.

AA treatment did not change the expression levels of αSMA and ALP of VICs encapsulated in PEG–PQ hydrogels. (A, B) Representative fluorescent images of αSMA staining of VICs encapsulated in (A) GM or (B) GM + AA for 21 days: red, αSMA; blue (DAPI), nuclei; green (phalloidin), actin. (C, D) Representative fluorescent images of ALP staining of VICs encapsulated in (C) GM or (D) or GM + AA for 28 days: red, ALP; blue (DAPI), nuclei; scale bars = 50 μm. (E) Relative fluorescence intensities of αSMA, ALP and DAPI; no significant difference by Student's t-test, n = 3

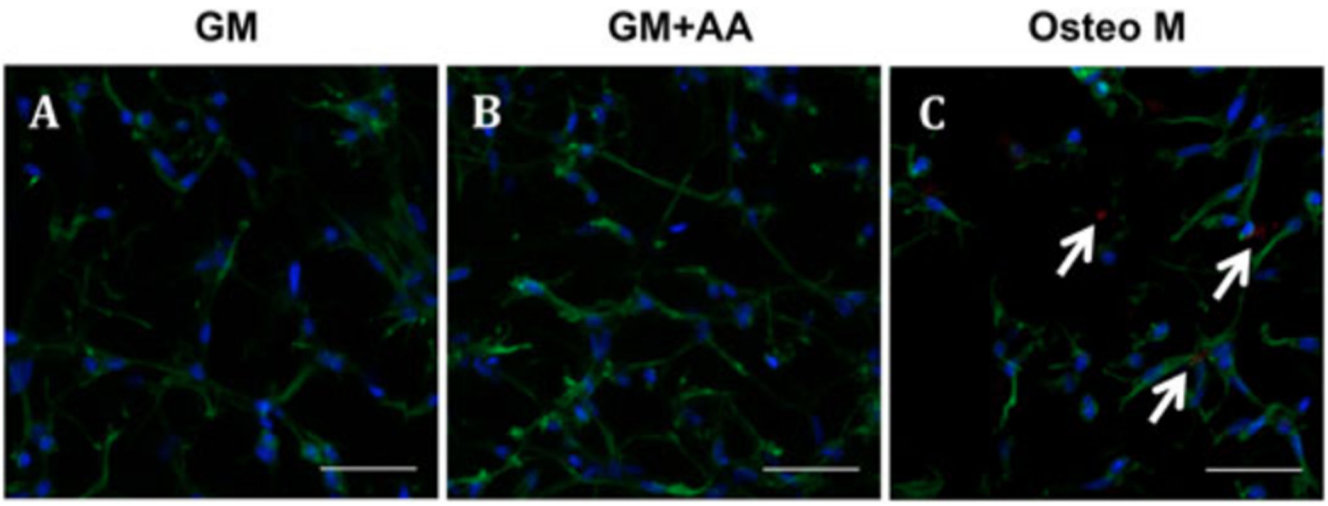

Figure 6.

Xylenol orange (calcification) was undetected in cell-laden hydrogels cultured in GM or GM + AA for 28 days, but was faintly detectable in those cultured in Osteo M: red (xylenol orange), calcium; blue (DAPI), nuclei; green (phalloidin), actin: representative fluorescent images of cell-laden hydrogels cultured in (A) GM, (B) GM + AA and (C) Osteo M; scale bars = 50 μm; white arrows, calcification

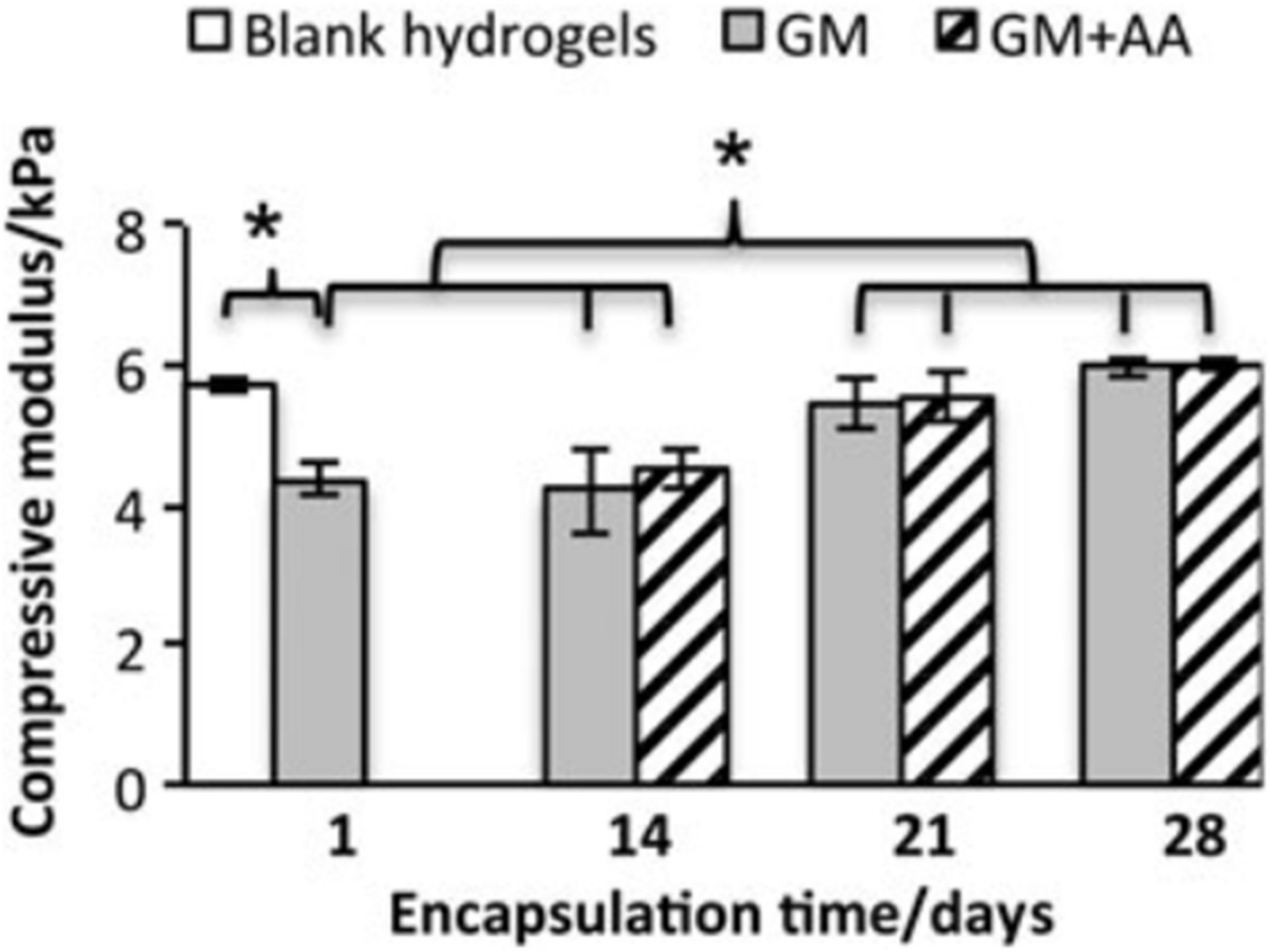

Figure 7.
Compressive moduli of cell-laden PEG–PQ hydrogels throughout the culture period of 28 days; *$p < 0.01$; $n = 4–6$